

6 March, 1995

Preprint PAR/LPTHE/95-09

hep-ph/9503326

A MODEL FOR THE DECAY OF THE D_s^+ MESON INTO THREE PIONS

M. Gourdin*, Y. Y. Keum[†] and X. Y. Pham*

Université Pierre & Marie Curie, Paris VI

Université Denis Diderot, Paris VII

Physique Théorique et Hautes Energies,

Unité associée au CNRS : D 0280

Abstract

We propose a phenomenological two component model describing the decay amplitude of the process $D_s^+ \rightarrow 3\pi$, whose rate has been found surprisingly large. The first component is a constant background F_{NR} , and the second one is a Breit-Wigner type amplitude associated to a quasi two body $f_0(980) \pi^+$ state. We show that it is possible to reproduce the observed rate for $D_s^+ \rightarrow \pi^+\pi^+\pi^-$ as well as the two other measured branching ratios for the non resonant part and the resonant $f_0\pi^+$ one, with a common parameter F_{NR} .

Predictions are given for the $D_s^+ \rightarrow \pi^0\pi^0\pi^+$ rates, as well as for the various π^+ and π^- , or π^0 and π^+ energy distributions for the two possible final states.

*Postal address: LPTHE, Tour 16, 1^{er} Etage, 4 Place Jussieu, F-75252 Paris CEDEX 05, France.

[†]Postal address: LPTHE, Tour 24, 5^{ème} Etage, 2 Place Jussieu, F-75251 Paris CEDEX 05, France.

E-mail : gourdin@lpthe.jussieu.fr, keum@lpthe.jussieu.fr, and pham@lpthe.jussieu.fr.

I Introduction

We are interested, in this paper, in the decay of the D_s^+ meson into three pions. We observe that both flavoured constituents c and \bar{s} of the D_s^+ meson are absent in the final state. As a consequence, the decay mode $D_s^+ \rightarrow 3 \pi$ can be described neither by a spectator, nor by a colour suppressed, nor by a penguin diagram, but only by a W annihilation where the virtual time-like W^+ decays into three pions.

It is generally expected that W annihilation amplitudes are small compared to spectator and colour suppressed ones. Surprisingly experimental data do not seem to support this belief. As an illustration, let us consider the three following decay modes of the D_s^+ meson involving the same Cabibbo, Kobayashi, Maskawa (CKM) factor $V_{cs}^* V_{ud}$ and compare their branching ratios [1] :

i) Spectator ;

$$Br(D_s^+ \rightarrow \phi + \pi^+) = (3.5 \pm 0.4) \% ,$$

ii) Colour suppressed ;

$$Br(D_s^+ \rightarrow \bar{K}^0 + K^+) = (3.5 \pm 0.7) \% ,$$

iii) W annihilation ;

$$Br(D_s^+ \rightarrow \pi^+ + \pi^+ + \pi^-) = (1.35 \pm 0.31) \% .$$

It is therefore interesting to understand the origin for such a large value of the $D_s^+ \rightarrow 3\pi$ branching ratio.

The transition of the virtual W into three pions occurs also in the τ decay mode $\tau^+ \rightarrow \bar{\nu}_\tau + 3\pi$. However, in this case, the full axial vector weak current contributes, and the amplitude depends on three independent structure functions. For the decay $D_s^+ \rightarrow 3\pi$, only one structure function associated to the divergence of the axial vector current is involved, because here the W is in the $J^P = O^-$ state, like the D_s meson. Therefore the study of $D_s \rightarrow 3\pi$ decay is the cleanest way to isolate the structure function F_4 of references [2, 3].

In Section II, we develop the formalism for $D_s^+ \rightarrow 3\pi$ decay. We study the kinematics and the three pion phase space. Experimental data as quoted in Reference [1] are listed.

By inspection of these experimental data, we observe that the quasi two body state $\rho^0 \pi^+$ assumed in [2, 3] to be responsible of the structure function F_4 is negligible compared to the quasi two body state $f_0(980) \pi^+$. Moreover, since the non resonant rate is large, we propose a model in Section III where

the decay amplitude for $D_s^+ \rightarrow 3\pi$ has two components : the first one is associated to a background non resonant three pions, and the second one corresponds to a quasi two body $f_0 \pi^+$ final state.

We compare our model with experiment in Section IV for the final state $\pi^+\pi^+\pi^-$ where data on rates are available and we make predictions for the π^+ and π^- energy distributions.

For the final state $\pi^0\pi^0\pi^+$, using isospin analysis, we make predictions in Section V for the rates and the π^0 and π^+ energy distributions.

Our model is consistent with the rate measurements. However the serious test would be the observation of the various π meson energy distributions and ultimately, if statistics is copious enough, of the Dalitz plots.

II Generalities and Kinematics

We study the decay of a D_s^+ meson of energy momentum P into three pions of energy momenta p_1, p_2, p_3 with the relation $P = p_1 + p_2 + p_3$. We introduce the Mandelstam variables s_1, s_2, s_3 and the π meson energies E_1, E_2, E_3 in the D_s^+ rest frame. Neglecting the mass difference between charged and neutral pions, we get

$$\begin{aligned} s_1 &= (p_2 + p_3)^2 = (P - p_1)^2 = m_{D_s}^2 + m_\pi^2 - 2m_{D_s}E_1 \quad , \\ s_2 &= (p_3 + p_1)^2 = (P - p_2)^2 = m_{D_s}^2 + m_\pi^2 - 2m_{D_s}E_2 \quad , \\ s_3 &= (p_1 + p_2)^2 = (P - p_3)^2 = m_{D_s}^2 + m_\pi^2 - 2m_{D_s}E_3 \quad . \end{aligned} \tag{1}$$

Energy momentum conservation implies the relations

$$s_1 + s_2 + s_3 = m_{D_s}^2 + 3m_\pi^2 \quad , \quad E_1 + E_2 + E_3 = m_{D_s} \quad . \tag{2}$$

The double differential distribution is given by

$$d\Gamma = \frac{1}{64} \frac{1}{\pi^3} \frac{1}{m_{D_s}} |\langle 3\pi | T | D_s^+ \rangle|^2 dE_1 dE_2 \quad , \tag{3}$$

and the transition matrix element $\langle 3\pi | T | D_s^+ \rangle$ involving only spinless particles is dimensionless.

In the (E_1, E_2) plane, the phase space is defined by the constraints

$$\begin{aligned} m_\pi &\leq E_1 \leq \frac{m_{D_s}^2 - 3m_\pi^2}{2m_{D_s}} \quad , \\ E_-(E_1) &\leq E_2 \leq E_+(E_1) \quad , \end{aligned} \tag{4}$$

with

$$E_\pm(E) = \frac{1}{2}(m_{D_s} - E) \pm \frac{1}{2} \left\{ \frac{(E^2 - m_\pi^2)(m_{D_s}^2 - 3m_\pi^2 - 2m_{D_s}E)}{m_{D_s}^2 + m_\pi^2 - 2m_{D_s}E} \right\}^{1/2} . \tag{5}$$

Of course, the mass difference between charged and neutral pions being neglected, we have the same phase space in the two other planes : (E_2, E_3) and (E_1, E_3) .

At the quark level, the decay $D_s^+ \rightarrow 3\pi$ is described by a W annihilation diagram, and the transition matrix element is given by

$$\langle 3\pi | T | D_s^+ \rangle = \frac{G_F}{\sqrt{2}} V_{cs}^* V_{ud} a_1 f_{D_s} P^\mu \langle 3\pi | A_\mu | 0 \rangle . \quad (6)$$

where a_1 is the phenomenological parameter introduced by Bauer, Stech, Wirbel [4], and f_{D_s} is the leptonic decay constant of the D_s meson. The matrix element of the divergence of the weak axial current between the vacuum and three pion final state is an unknown form factor $F(E_1, E_2)$, function of two independent variables, taken as the pion energies.

$$P^\mu \langle 3\pi | A_\mu | 0 \rangle = m_{D_s} F(E_1, E_2) . \quad (7)$$

Since the transition matrix element is dimensionless, the form factor $F(E_1, E_2)^\dagger$ is also dimensionless.

In the (E_1, E_2) plane, the Dalitz plot is given by :

$$d\Gamma(D_s^+ \rightarrow 3\pi) = \frac{m_{D_s}}{64 \pi^3} \left(\frac{G_F}{\sqrt{2}} \right)^2 |V_{cs}|^2 |V_{ud}|^2 a_1^2 f_{D_s}^2 |F(E_1, E_2)|^2 dE_1 dE_2 . \quad (8)$$

The decay rate is obtained by integration of the distribution (8) over the energies E_1 and E_2 inside the phase space described in Eq.(4). The branching ratio can be written in the form :

$$Br(D_s^+ \rightarrow 3\pi) = \frac{\tau_{D_s^+} m_{D_s}}{\hbar} \frac{1}{64 \pi^3} \left[\frac{G_F m_{D_s}^2}{\sqrt{2}} \right]^2 |V_{cs}|^2 |V_{ud}|^2 a_1^2 \left(\frac{f_{D_s}}{m_{D_s}} \right)^2 I , \quad (9)$$

where the dimensionless integral I is defined by :

$$I = \frac{1}{m_{D_s}^2} \int \int |F(E_1, E_2)|^2 dE_1 dE_2 . \quad (10)$$

Using $\tau_{D_s^+} = 4.67 \cdot 10^{-13} s$ [1] and $f_{D_s} = 280 MeV$ [§], we get

$$Br(D_s^+ \rightarrow 3\pi) = 1.31 \cdot 10^{-2} a_1^2 I . \quad (11)$$

From the analysis of colour favoured D meson decay, a reasonable value for a_1 is $a_1 = 1.26$ [5] and we obtain

$$Br(D_s^+ \rightarrow 3\pi) = 2.08 \cdot 10^{-2} I . \quad (12)$$

[†]Our $F(E_1, E_2)$ is related to the F_4 of the Ref.[2] by $F(E_1, E_2) = m_{D_s} F_4(s_1, s_2, Q^2 = m_{D_s}^2)$

[§]The leptonic decay $D_s^+ \rightarrow \mu^+ + \nu_\mu$ has been measured by two groups and the extracted values of f_{D_s} are $f_{D_s} = (232 \pm 69) MeV$ and $f_{D_s} = (344 \pm 76) MeV$. Our choice of $f_{D_s} = 280 MeV$ is consistent with data and with theoretical expectations.

We make the following choice of π -meson energy variables ;

- i) final state $\pi^+\pi^+\pi^-$ $E_1(\pi^+), E_2(\pi^+), E_3(\pi^-)$,
- ii) final state $\pi^0\pi^0\pi^+$ $E_1(\pi^0), E_2(\pi^0), E_3(\pi^+)$.

Due to Bose-Einstein symmetry, the function $F(E_1, E_2)$ is symmetrical in the exchange between E_1 and E_2 . Such a property extends to the Dalitz plot given by the double differential distribution represented by $|F(E_1, E_2)|^2$. It is probably premature to discuss the details of the Dalitz plot and it might be interesting to define one meson energy distributions :

$$G(E_1) = \frac{1}{m_{D_s}} \int_{E_-(E_1)}^{E_+(E_1)} |F(E_1, E_2)|^2 dE_2 , \quad (13)$$

$$H(E_3) = \frac{1}{m_{D_s}} \int_{E_-(E_3)}^{E_+(E_3)} |F(m_{D_s} - E_2 - E_3, E_2)|^2 dE_2 , \quad (14)$$

where $G(E_1)$ corresponds to the $\pi^+(\pi^0)$ for the final state $\pi^+\pi^+\pi^-(\pi^0\pi^0\pi^+)$, and $H(E_3)$ corresponds to the $\pi^-(\pi^+)$ for the final state $\pi^+\pi^+\pi^-(\pi^0\pi^0\pi^+)$.

The presently available data concern the rates for the decay mode $D_s^+ \rightarrow \pi^+\pi^+\pi^-$. They are given in Table 1, the last column indicates the value of the quantity I determined from experiment [1] by using Eq.(12).

Mode	Experimental Branching Ratios	Experimental values of I
$\pi^+\pi^+\pi^-$	$(1.35 \pm 0.31) \cdot 10^{-2}$	0.649 ± 0.149
$(\pi^+\pi^+\pi^-)_{NR}$	$(1.01 \pm 0.35) \cdot 10^{-2}$	0.486 ± 0.168
$f_0\pi^+$	$(1 \pm 0.4) \cdot 10^{-2}$	0.481 ± 0.192
$\rho^0\pi^+$	$\leq 0.28 \cdot 10^{-2}$	≤ 0.135

Table 1

III. Phenomenological Model for $D_s^+ \rightarrow 3\pi$

In order to describe the decay mode $D_s^+ \rightarrow 3\pi$, we use a simple phemonenological model where the function $F(E_1, E_2)$ is the sum of two contributions ;

$$F(E_1, E_2) = F_{NR} + F_{RES}(E_1, E_2) . \quad (15)$$

Obviously, this decomposition is guided by experimental data [1]. The first component F_{NR} is assumed to be a real constant describing the non resonant part of the amplitude. The second component

$F_{RES}(E_1, E_2)$ is associated to the quasi two body final state $D_s^+ \rightarrow f_0 + \pi^+$ followed by the subsequent decays $f_0 \rightarrow \pi^+\pi^-$ or $\pi^0\pi^0$.

1). At first, consider the charged case $f_0 \rightarrow \pi^+\pi^-$. The π^- meson has an energy E_3 and the two π^+ mesons energies E_1 and E_2 . We then have two possible resonant combinations and the general form of $F_{RES}(E_1, E_2)$ is :

$$F_{RES}(E_1, E_2) = D_c \{BW(E_1) + BW(E_2)\} , \quad (16)$$

where the dimensionless Breit-Wigner function $BW(E_j)$ is defined by :

$$BW(E_j) = \frac{m_{f_0}^2}{m_{f_0}^2 - s_j - i\sqrt{s_j} \Gamma_{f_0}} \quad (17)$$

with s_j and E_j related by $s_j = m_{D_s}^2 + m_\pi^2 - 2m_{D_s}E_j$ ($j = 1, 2$).

The complex constant D_c corresponds to the transition $W^+ \rightarrow f_0\pi^+$, for which we assume, by the Partial Conservation of the Axial Current (PCAC) in Eqs.(6) and (7), the existence of an intermediate state having the quantum number of a π^+ meson [2, 3, 6] and which might be the π meson itself or its recurrence $\pi(1300)$. It turns out that the π meson intermediate state will give a contribution many order of magnitude smaller than that of the $\pi(1300)$ and only the later one is retained given the following expression for D_c ¶ :

$$D_c = \frac{m_{D_s}}{m_{f_0}} \frac{f_{\pi'} m_{\pi'}}{m_{\pi'}^2 - m_{D_s}^2 - i m_{D_s} \Gamma_{\pi'}} g_{\pi' f_0 \pi} g_{f_0 \pi^+ \pi^-} . \quad (18)$$

In Eq.(18), $\pi' \equiv \pi(1300)$, and the dimensionless coupling constants $g_{M_0 M_1 M_2}$ describe the decay of a spinless meson M_0 into two spinless mesons M_1 and M_2 :

$$\langle M_1 M_2 | T | M_0 \rangle = m_0 g_{M_0 M_1 M_2} . \quad (19)$$

The term m_{D_s} in the numerator of Eq.(18) comes from the definition Eq.(7), the term m_{f_0} in the denominator of Eq.(18) when combined with Eq.(17) yields the definition Eq.(19). Also $m_{\pi'}$ comes from Eq.(19) and $f_{\pi'}$ comes from the coupling between π' and W . The numerical value of $g_{M_0 M_1 M_2}$ is obtained from the experimental decay rate $\Gamma(M_0 \rightarrow M_1 + M_2)$ by the relation

$$g_{M_0 M_1 M_2}^2 = 8 \pi \frac{\Gamma(M_0 \rightarrow M_1 + M_2)}{K} , \quad (20)$$

where K is the final momentum in the M_0 rest frame.

¶ We have used for width the simple energy dependence $\Gamma(s) = \frac{\sqrt{s}}{m} \Gamma(m)$. In the case of the $\pi(1300)$ width, more sophisticated dependence has been proposed [2]. Because of the not too large difference between the $\pi(1300)$ and D_s^+ masses, we expect the sensitivity of Eq.(18) to different forms of $\Gamma_{\pi'}(s)$ to be relatively modest.

Now we consider first the case $f_0 \rightarrow 2\pi$. Using the experimental parameters [1] :

$$\begin{aligned} m_{f_0} &= 980 \text{ MeV} \quad , \quad \Gamma_{f_0} = (49 \pm 9) \text{ MeV} \quad , \\ Br(f_0 \rightarrow 2\pi) &= 0.781 \pm 0.024 \quad , \end{aligned} \quad (21)$$

we obtain

$$g_{f_0\pi^+\pi^-} = 1.144 \pm 0.109 \quad , \quad g_{f_0\pi^0\pi^0} = 0.809 \pm 0.077 \quad . \quad (22)$$

The isoscalar property of the f_0 meson has been taken into account for relating both coupling constants.

Secondly, for the decay $\pi(1300) \rightarrow f_0 + \pi$, experimental data are poor [1] and we shall use :

$$\begin{aligned} m_{\pi'} &= 1300 \text{ MeV} \quad , \quad \Gamma_{\pi'} = (400 \pm 200) \text{ MeV} \quad , \\ Br(\pi' \rightarrow f_0\pi) &= 0.68 \quad . \end{aligned} \quad (23)$$

The result is

$$g_{\pi' f_0 \pi} = 5.2^{+1.2}_{-1.5} \quad . \quad (24)$$

The last parameter entering in Eq.(18) is the leptonic constant $f_{\pi'}$. The estimate of reference [6] is ^{||}

$$f_{\pi'} = 40 \text{ MeV} \quad (25)$$

Now we are in a position to compute the numerical value of the dimensionless coupling constant D_c written in the form $D_c = |D_c| \exp(i \Phi_D)$. Retaining only the large error due to the poor knowledge of the total $\pi(1300)$ width, we obtain for different $\Gamma_{\pi'}$ values :

$$\Gamma_{\pi'} = \begin{vmatrix} 600 \\ 400 \\ 200 \end{vmatrix} \text{ MeV} \quad , \quad |D_c| = \begin{vmatrix} 0.3068 \\ 0.2679 \\ 0.1981 \end{vmatrix} \quad , \quad \Phi_D = \begin{vmatrix} 152^\circ \\ 160^\circ \\ 170^\circ \end{vmatrix} \quad (26)$$

2). In the second case $f_0 \rightarrow \pi^0\pi^0$, we call E_1 and E_2 the energies of the π^0 's and E_3 the energy of the π^+ . The general form of $F_{RES}(E_1, E_2)$ is

$$F_{RES}(E_1, E_2) = D_N \text{ BW}(E_3) \quad , \quad (27)$$

and because of Eq.(22), $D_N = D_c/\sqrt{2}$.

IV. Results of the model for $D_s^+ \rightarrow \pi^+\pi^+\pi^-$

The results of the model for the one pion energy distributions and for the rates are now given in the three following cases :

^{||}Different values of $f_{\pi'}$ have been proposed in the literature. See for instance references [2] and [3].

- 1) non resonant $\pi^+\pi^+\pi^-$ state : F_{NR}
- 2) quasi two body $f_0\pi^+ \rightarrow \pi^+\pi^-\pi^+$ state : F_{RES}
- 3) superposition of the non resonant and resonant amplitudes : $F_{NR} + F_{RES}$

1). In the non resonant case, we have an uniform Dalitz plot and for a constant F_{NR} , we get from Eqs.(13) and (14) :

$$G_{NR}(E) = H_{NR}(E) = F_{NR}^2 \frac{1}{m_{D_s}} \left\{ \frac{(E^2 - m_\pi^2)(m_{D_s}^2 - 3m_\pi^2 - 2m_{D_s}E)}{m_{D_s}^2 + m_\pi^2 - 2m_{D_s}E} \right\}^{1/2} . \quad (28)$$

Here E stands for E_1, E_2, E_3 indifferently.

The energy distribution is represented on Figure 1 for $F_{NR} = 1$. The integral I_{NR} given by

$$I_{NR} = \frac{1}{m_{D_s}} \int_{m_\pi}^{\frac{m_{D_s}^2 - 3m_\pi^2}{2m_{D_s}}} G_{NR}(E) dE , \quad (29)$$

has the numerical value **

$$I_{NR} = 0.1053 F_{NR}^2 . \quad (30)$$

Using, for I_{NR} , the experimental value quoted in Table 1 in the non resonant case, we obtain

$$|F_{NR}| = 2.15 \pm_{0.41}^{0.34} . \quad (31)$$

2). Now we consider the quasi two body case $D_s^+ \rightarrow f_0 + \pi^+ \rightarrow \pi^+\pi^-\pi^+$ for which the amplitude F_{RES} is given by Eq.(16). It is convenient to write

$$|F_{RES}(E_1, E_2)|^2 = |D_c|^2 K_c(E_1, E_2) , \quad (32)$$

where the function $K_c(E_1, E_2)$ is the sum of three terms ;

$$K_c(E_1, E_2) = |BW(E_1)|^2 + |BW(E_2)|^2 + 2Re \{ BW(E_1)BW(E_2)^* \} . \quad (33)$$

After integration of $K_c(E_1, E_2)$ over E_2 at fixed E_1 , as indicated in Eq.(13), we obtain the π^+ meson energy distribution in the form :

$$G_{RES}(E_1) = |D_c|^2 K_c^{(+)}(E_1) . \quad (34)$$

The function $K_c^{(+)}(E_1)$ is represented on Figure 2. Clearly we see the narrow peak due to the Breit-Wigner term in E_1 and a quasi-constant background corresponding to the Breit-Wigner term in E_2 . The interference between the two Breit-Wigner terms gives a very small contribution to $K_c^{(+)}(E_1)$.

**In the limit $m_\pi = 0$, the calculation of I_{NR} is trivial and the result is $I_{NR} = 0.125 F_{NR}^2$. Correction due to $m_\pi \neq 0$ is large and of the order of 16% in spite of the very small value of $m_\pi/m_{D_s} \simeq 0.07$.

Integrating now $K_c(E_1, E_2)$ over E_2 at fixed E_3 , as indicated in Eq.(14), we obtain the π^- meson energy distribution :

$$H_{RES}(E_3) = |D_c|^2 K_c^{(-)}(E_3) . \quad (35)$$

The function $K_c^{(-)}(E_3)$ is also represented on Figure 2. The result is a quasi-constant plateau in most of the allowed phase space domain of E_3 .

In order to obtain the rate, we must perform a second energy integration. The quantity I_{RES} is written in the form :

$$I_{RES} = |D_c|^2 K_c , \quad (36)$$

where K_c is given by :

$$K_c = \frac{1}{m_{D_s}} \int_{m_\pi}^{\frac{m_{D_s}^2 - 3m_\pi^2}{2m_{D_s}}} K_c^{(+)}(E_1) dE_1 = \frac{1}{m_{D_s}} \int_{m_\pi}^{\frac{m_{D_s}^2 - 3m_\pi^2}{2m_{D_s}}} K_c^{(-)}(E_3) dE_3 . \quad (37)$$

The numerical value obtained for K_c is $K_c = 5.7217$.

Using now the results of Eq.(26) for $|D_c|$, we obtain the numerical value in our model of I_{RES} defined in Eq.(36). The result is

$$I_{RES} = 0.411 \pm_{0.186}^{0.128} , \quad (38)$$

where, as previously explained, the errors correspond to $\Gamma_{\pi'} = 400 \pm 200 MeV$.

The theoretical value of I_{RES} in Eq.(38) is consistent with the measured value of 0.481 ± 0.192 quoted in Table 1. If we consider seriously the experimental one standard deviation limit, $I_{RES} \geq 0.289$, we get a lower bound for $\Gamma_{\pi'}$, $\Gamma_{\pi'} \geq 263 MeV$ (assuming $f_{\pi'} = 40 MeV$). There is no upper bound constraint on $\Gamma_{\pi'}$.

3). Finally we consider the full amplitude written in Eq.(15). As the constant F_{NR} is real, we get

$$|F(E_1, E_2)|^2 = F_{NR}^2 + 2 F_{NR} Re \{ F_{RES}(E_1, E_2) \} + |F_{RES}(E_1, E_2)|^2 . \quad (39)$$

We integrate over E_1 and E_2 in order to obtain the quantity I of Eq.(10).

Using the previous results Eqs.(30) and (36), we obtain

$$I = 0.1053 F_{NR}^2 + 2 F_{NR} |D_c| |J| Cos(\Phi_D + \Phi_J) + 5.7217 |D_c|^2 , \quad (40)$$

where the complex integral J is defined by :

$$J = \frac{1}{m_{D_s}^2} \int \int \{ BW(E_1) + BW(E_2) \} dE_1 dE_2 = |J| e^{i\Phi_J} . \quad (41)$$

The results are

$$|J| = 0.2677 , \quad \Phi_J = 89.60^\circ . \quad (42)$$

Using the experimental constraints for I_{NR} and I given in Table 1, from Eqs.(30) and (40), we can check the consistency of our model by determining the parameter F_{NR} and compare to Eq.(31). The results are presented on Table 2 for three value of $\Gamma_{\pi'}$, $\Gamma_{\pi'} = 600, 400, 263 \text{ MeV}$. For large value of $\Gamma_{\pi'}$, we obtain only positive solutions for F_{NR} . When $\Gamma_{\pi'}$ decreases, $|D_c|$ decreases and the interference term in Eq.(40) becomes smaller, then we obtain both positive and negative solutions for F_{NR} .

$\Gamma_{\pi'} \text{ (MeV)}$	F_{NR}		I_{NR}		I		I_{RES}
600	1.7378	1.9898	0.318	0.417	0.719	0.798	0.5385
400	1.7378	2.1680	0.318	0.495	0.642	0.798	0.4105
263	1.7378	2.3385	0.318	0.576	0.557	0.798	0.2890
	-1.7378	-2.0671	0.318	0.456	0.657	0.798	0.2890
Experiment	—		0.318 — 0.654		0.500 — 0.798		0.289 — 0.673

Table 2

The full pion energy distributions coming from the total amplitude in Eq.(39) depend on the two quantities F_{NR} and D_c . Writing the squared modulus of the total amplitude in the form :

$$|F(E_1, E_2)|^2 = F_{NR}^2 + 2F_{NR} \text{Re} \{D_c J_c(E_1, E_2)\} + |D_c|^2 K_c(E_1, E_2) \quad , \quad (43)$$

where $K_c(E_1, E_2)$ is given by Eq.(33) and $J_c(E_1, E_2)$ is simply given by :

$$J_c(E_1, E_2) = BW(E_1) + BW(E_2) \quad . \quad (44)$$

Of course, $K_c(E_1, E_2) = |J_c(E_1, E_2)|^2$.

After integration of Eq.(43) over E_2 at fixed E_1 , we obtain the π^+ meson energy distribution $G_c(E_1)$:

$$G_c(E_1) = F_{NR}^2 G_{NR}(E_1) + 2 F_{NR} \text{Re} \{D_c J_c^+(E_1)\} + |D_c|^2 K_c^+(E_1) \quad . \quad (45)$$

The quantities $G_{NR}(E_1)$ and $K_c^+(E_1)$ have been represented on Figures 1 and 2, respectively, and $J_c^+(E_1)$ is defined by :

$$J_c^+(E_1) = \frac{1}{m_{D_s}} \int_{E_-(E_1)}^{E_+(E_1)} J_c(E_1, E_2) dE_2 \quad . \quad (46)$$

In a similar way, integrating over E_2 at fixed E_3 , we obtain the π^- meson energy distribution in the form :

$$H_c(E_3) = F_{NR}^2 G_{NR}(E_3) + 2 F_{NR} \text{Re} \{D_c J_c^-(E_3)\} + |D_c|^2 K_c^-(E_3) \quad . \quad (47)$$

In Eq.(47), $G_{NR}(E_3)$ as given by Eq.(28) is represented on Figure 1. The quantity $K_c^-(E_3)$ is represented on Figure 2 and $J_c^-(E_3)$ is defined by :

$$J_c^-(E_3) = \frac{1}{m_{D_s}} \int_{E_-(E_3)}^{E_+(E_3)} J_c(m_{D_s} - E_2 - E_3, E_2) dE_2 \quad . \quad (48)$$

As mentioned above, the full π^+ and π^- energy distributions $G_c(E_1)$ and $H_c(E_3)$ are functions of F_{NR} and D_c . They are represented respectively in Figures 3 and 4.

V. Prediction of the model for $D_s^+ \rightarrow \pi^0 \pi^0 \pi^+$

We have no experimental data on the decay mode $D_s^+ \rightarrow \pi^0 \pi^0 \pi^+$. However our model can make predictions for the three following cases :

- 1) non resonant $\pi^0 \pi^0 \pi^+$ state,
- 2) quasi two body $f_0 \pi^+ \rightarrow \pi^0 \pi^0 \pi^+$ state,
- 3) superposition of the non resonant and resonant amplitude.

1). In the non resonant case of a constant function $F_{NR}(E_1, E_2)$, we obtain the same shape for one pion energy distribution as shown on Figure 1.

However the constant F_{NR} has no reason to be the same for the two modes $\pi^+ \pi^+ \pi^-$ and $\pi^0 \pi^0 \pi^-$. We now discuss this problem. By assumption, with a constant function $F_{NR}(E_1, E_2)$, we have a full symmetry in space between the three pions. From the Bose-Einstein symmetry, the isospin configuration has also to be totally symmetric. Consider now a third rank fully symmetric tensor in a 3 dimensional space. It has 10 independent components. With respect to the isospin $SO(3)$ orthogonal group, such a tensor is reducible into an isospin $I = 3$ part with 7 components and an isospin $I = 1$ part with 3 components. In our specific problem, only the later part contributes, the $u\bar{d}$ weak current being an isovector. By inspection of the relevant Clebsch-Gordan coefficients, we obtain the result :

$$F_{NR}(\pi^+ \pi^+ \pi^-) = 3 F_{NR}(\pi^0 \pi^0 \pi^+) \quad . \quad (49)$$

As a consequence, in our model, we obtain for the non resonant part :

$$\frac{\Gamma(D_s^+ \rightarrow \pi^0 \pi^0 \pi^+)_{NR}}{\Gamma(D_s^+ \rightarrow \pi^+ \pi^+ \pi^-)_{NR}} = 11.1 \quad \% \quad , \quad (50)$$

and the non resonant branching ratio $Br(D_s^+ \rightarrow \pi^0 \pi^0 \pi^+)_{NR}$ is expected to occur only at the 10^{-3} level.

2). For the quasi two body decay of $D_s^+ \rightarrow f_0 \pi^+ \rightarrow \pi^0 \pi^0 \pi^+$, the amplitude F_{RES} is given by Eq.(27) :

$$|F_{RES}(E_1, E_2)|^2 = |D_N|^2 K_N(E_1, E_2) \quad (51)$$

where the function $K_N(E_1, E_2)$ is simply given by :

$$K_N(E_1, E_2) = |BW(E_3)|^2 = |BW(m_{D_s} - E_1 - E_2)|^2 \quad (52)$$

After integration over E_2 at fixed E_1 , as indicated in Eq.(13), we obtain the π^0 meson energy distribution in the form :

$$G_{RES}(E_1) = |D_N|^2 K_N^{(0)}(E_1) \quad (53)$$

The function $K_N^{(0)}(E_1)$ is a quasi flat distribution represented on Figure 5.

Integrating now over E_2 at fixed E_3 , as indicated in Eq.(14), we have the π^+ energy distribution in the form :

$$H_{RES}(E_3) = |D_N|^2 K_N^{(+)}(E_3) \quad (54)$$

The function $K_N^{(+)}(E_3)$ is represented on Figure 5 and the result exhibits a narrow Breit-Wigner peak similar to the one drawn on Figure 2 for $K_c^+(E_1)$.

The decay rate is now obtained by performing a second energy integration. The quantity I_{RES} is written in the form :

$$I_{RES} = |D_N|^2 K_N \quad , \quad (55)$$

where K_N is given by :

$$K_N = \frac{1}{m_{D_s}} \int_{m_\pi}^{\frac{m_{D_s}^2 - 3m_\pi^2}{2m_{D_s}}} K_N^{(0)}(E_1) dE_1 = \frac{1}{m_{D_s}} \int_{m_\pi}^{\frac{m_{D_s}^2 - 3m_\pi^2}{2m_{D_s}}} K_N^{(+)}(E_3) dE_3 \quad (56)$$

The numerical value of K_N is $K_N = 2.7469$.

Using the relation between D_N and D_c , we make the prediction

$$\frac{\Gamma(D_s^+ \rightarrow f_0 \pi^+ \rightarrow \pi^0 \pi^0 \pi^+)}{\Gamma(D_s^+ \rightarrow f_0 \pi^+ \rightarrow \pi^+ \pi^- \pi^+)} = 24 \% \quad (57)$$

The departure of this ratio from 25 % is simply due to the interference between the two Breit-Wigner contributions in $D_s^+ \rightarrow f_0 \pi^+ \rightarrow \pi^+ \pi^- \pi^+$.

3). We finally consider the full amplitude written in the form of Eq.(15). An equation similar to Eq.(40) gives the total rate, and going from the mode $\pi^+ \pi^+ \pi^-$ to the mode $\pi^0 \pi^0 \pi^+$ implies the changes :

$$F_{NR} \rightarrow \frac{1}{3} F_{NR} \quad , \quad D_c \rightarrow \frac{1}{\sqrt{2}} D_c \quad , \quad J \rightarrow \frac{1}{2} J \quad , \quad K_c \rightarrow K_N \quad (58)$$

and we obtain instead of Eq.(40) :

$$I_{\pi^0 \pi^0 \pi^+} = 0.0117 F_{NR}^2 + 0.2357 F_{NR} |D_c| |J| \cos(\Phi_D + \Phi_J) + 1.3735 |D_c|^2 \quad . \quad (59)$$

Using the solutions for F_{NR} given in the Table 2, we can compute the decay rate for the $\pi^0\pi^0\pi^+$ mode as a function of F_{NR} and of the π' width $\Gamma_{\pi'}$ via the quantity D_c . In Table 3, we show the results for the ratio R defined by :

$$R = \frac{\Gamma(\pi^0\pi^0\pi^+)}{\Gamma(\pi^+\pi^+\pi^-)} . \quad (60)$$

$\Gamma_{\pi'}$ (MeV)	F_{NR}		R
600	1.7378	1.9898	20.2 ± 0.5 %
400	1.7378	2.1680	18.5 ± 0.8 %
263	1.7378	2.3385	16.7 ± 1 %
	-1.7378	-2.0671	16.3 ± 0.5 %

Table 3

The pion energy distributions depend on F_{NR} and D_c , and we have for the squared amplitude an expression similar to Eq.(43) with the appropriated changes indicated on Eq.(58) :

$$|F(E_1, E_2)|^2 = \frac{1}{9}F_{NR}^2 + \frac{2}{3\sqrt{2}}F_{NR}Re\{D_c J_N(E_1, E_2)\} + \frac{1}{2}|D_c|^2 K_N(E_1, E_2) , \quad (61)$$

where $J_N(E_1, E_2)$ contains only one Breit-Wigner amplitude :

$$J_N(E_1, E_2) = BW(E_3) = BW(m_{D_s} - E_1 - E_2) , \quad (62)$$

and $K_N(E_1, E_2) = |J_N(E_1, E_2)|^2$.

The full π^0 energy distribution is obtained after integration of $|F(E_1, E_2)|^2$ over E_2 at fixed E_1 , and the full π^+ energy distribution after intergration over E_2 at fixed E_3 :

$$G_N(E_1) = \frac{1}{9}F_{NR}^2 G_{NR}(E_1) + \frac{2}{3\sqrt{2}}F_{NR}Re\{D_c J_N^{(0)}(E_1)\} + \frac{1}{2}|D_c|^2 K_N^{(0)}(E_1) , \quad (63)$$

$$H_N(E_3) = \frac{1}{9}F_{NR}^2 G_{NR}(E_3) + \frac{2}{3\sqrt{2}}F_{NR}Re\{D_c J_N^{(+)}(E_3)\} + \frac{1}{2}|D_c|^2 K_N^{(+)}(E_3) , \quad (64)$$

The functions $K_N^{(0)}(E_1)$ and $K_N^{+}(E_3)$ have been represented on Figure 5. The functions $J_N^{(0)}$ and $J_N^{(+)}$ are defined by :

$$J_N^{(0)}(E_1) = \frac{1}{m_{D_s}} \int_{E_-(E_1)}^{E_+(E_1)} BW(m_{D_s} - E_1 - E_2) dE_2 , \quad (65)$$

$$J_N^{(+)}(E_3) = \frac{1}{m_{D_s}} \int_{E_-(E_3)}^{E_+(E_3)} BW(E_3) dE_2 , \quad (66)$$

The π^0 and π^+ energy distributions $G_N(E_1)$ and $H_N(E_3)$ are functions of F_{NR} and D_c . They are represented on Figures 6 and 7 with the same values for $\Gamma_{\pi'}$ and F_{NR} as those used in Figures 3 and 4. The first observation is the minor role now played by the constant non resonant component essentially due to the isospin factor Eq.(49). However the sign of the interference between the two components can be observed at large values of E_3 as illustrated in Figures 7-a and 7-b.

V. Summary and Concluding Remarks

The large value experimentally observed for the branching ratio of the decay mode $D_s^+ \rightarrow \pi^+\pi^+\pi^-$ is a very interesting problem which necessitates a better understanding of the role played by the W annihilation mechanism in D meson decay, and which is probably more important than usually expected.

We have proposed to construct the unique structure function $F(E_1, E_2)$ as the sum of a constant non resonant term described by a real parameter F_{NR} , and a Breit-Wigner resonant term associated to a quasi two body $f_0(980) + \pi^+$ state which seems to play an important role as indicated by experiments. The quasi two body $\rho^0 + \pi$ state which is commonly considered by previous authors [2, 3, 6] is experimentally depressed and has been disregarded here.

It is possible to determine the resonant amplitude using parameters experimentally known, even if a large uncertainty remains on their precise experimental values. We have only retained, for simplicity, the uncertainty due to the $\pi(1300)$ width. Our model depends only on one free parameter, and we show that it is possible to find values of F_{NR} fitting the three observed rates : total $D_s^+ \rightarrow \pi^+\pi^+\pi^-$, non resonant $(D_s^+ \rightarrow \pi^+\pi^+\pi^-)_{NR}$, and resonant $D_s^+ \rightarrow f_0\pi^+ \rightarrow \pi^+\pi^+\pi^-$. This result is obviously non trivial.

Of course, the Dalitz plots are determined by the squared modulus of the structure function $|F(E_1, E_2)|^2$ and they are predicted by our model. Before the double differential quantities could be observed for the reason of statistics, it would be easier to measure the one pion energy distributions which are nothing but projections of the Dalitz plots on one energy axis. The figures shown in this paper present the various situations to be compared with experimental results when available.

The decay mode $D_s^+ \rightarrow \pi^0\pi^0\pi^+$ has not been experimentally observed, however the rates, the pion energy distributions, and the Dalitz plots can be computed in our model. We compare the $\pi^0\pi^0\pi^+$ and $\pi^+\pi^+\pi^-$ integrated widths through the ratio R in Eq.(60) and Table 3, and we also draw the π^0 and π^+ meson energy distributions. The quantity R is predicted to be in the 16% – 20% range and that might be the reason why the mode $D_s^+ \rightarrow \pi^0\pi^0\pi^+$ has not yet been detected, its branching ratio being expected to be few 10^{-3} .

We wish to emphasize that in the absence of additional experimental informations, our crude model is the simplest one accounting for the observed rates. In particular, for the resonant component, the normalization is estimated theoretically and constrained experimentally. Fortunately both approaches overlap, a fact a priori not evident, and they can be improved when experimental uncertainty will be reduced.

Acknowledgements

Y. Y. K would like to thank the Commissariat à l'Energie Atomique of France for the award of a fellowship and especially G. Cohen-Tannoudji and J. Haïssinski for their encouragements.

References

- [1] Review of Particles Properties, Reference as Phys. Rev. **D 50**, August 1994.
- [2] J. H. Kühn and E. Mirkes, *Phys. Lett.* **B 286** 381 (1992); *Z. Phys.* **C 56** 661 (1992).
- [3] J. Stern, N. H. Fuchs and M. Knecht, Proceedings of the 3rd Workshop on the τ -Charm factory, Preprint IPN/TH 93-38.
- [4] M. Wirbel, B. Stech and M. Bauer, *Z. Phys.* **C29** 637 (1985);
M. Bauer, B. Stech and M. Wirbel, *Z. Phys.* **C34** 103 (1987).
- [5] M. Neubert, V. Rieckert, B. Stech and Q. P. Xu, Advanced Series on Directions in High Energy Physics Vol. 10, Heavy Flavours, page 286, Editors A.J. Buras and M. Lindner, (World Scientific, Singapore, 1992).
- [6] N. Isgur, C. Morningstar and C. Reader, *Phys. Rev.* **D 39** 1357 (1989)

Figure captions

1. **Figure 1 :** The shape of the pion energy distributions for a uniform Dalitz plot. E stands for E_1, E_2, E_3 indifferently.
2. **Figure 2 :** The shapes of the π^+ and π^- meson energy distributions for $D_s^+ \rightarrow f_0 \pi^+ \rightarrow \pi^+ \pi^- \pi^+$. $K_c^+(E)$ represents the energy distribution of π^+ meson and $K_c^-(E)$ represents that of π^- meson. The quantity $E_0 = 7.45 \text{ GeV}$ is associated to the f_0 resonance.
3. **Figure 3 :** The fully normalized π^+ meson energy distribution for $D_s^+ \rightarrow \pi^+ \pi^- \pi^+$.

$$3\text{-a) for } \Gamma_{\pi'} = 600 \text{ MeV}, \quad 1.74 \leq F_{NR} \leq 1.99$$

$$3\text{-b) for } \Gamma_{\pi'} = 263 \text{ MeV}, \quad -2.07 \leq F_{NR} \leq -1.74$$

The two lines in each curve correspond to the extremum values of F_{NR} . The quantity $E_0 = 7.45 \text{ GeV}$ is associated to the f_0 resonance.

4. **Figure 4 :** The fully normalized π^- meson energy distribution for $D_s^+ \rightarrow \pi^+ \pi^- \pi^+$. The parameters are the same as in Figure 3.
5. **Figure 5 :** The shapes of the π^0 and π^+ meson energy distributions for $D_s^+ \rightarrow f_0 \pi^+ \rightarrow \pi^0 \pi^0 \pi^+$. The quantity $E_0 = 7.45 \text{ GeV}$ is associated to the f_0 resonance.
6. **Figure 6 :** The fully normalized π^0 meson energy distribution for $D_s^+ \rightarrow \pi^0 \pi^0 \pi^+$. The parameters are the same as in Figure 3.
7. **Figure 7 :** The fully normalized π^+ meson energy distribution for $D_s^+ \rightarrow \pi^0 \pi^0 \pi^+$. The parameters are the same as in Figure 3. The quantity $E_0 = 7.45 \text{ GeV}$ is associated to the f_0 resonance.

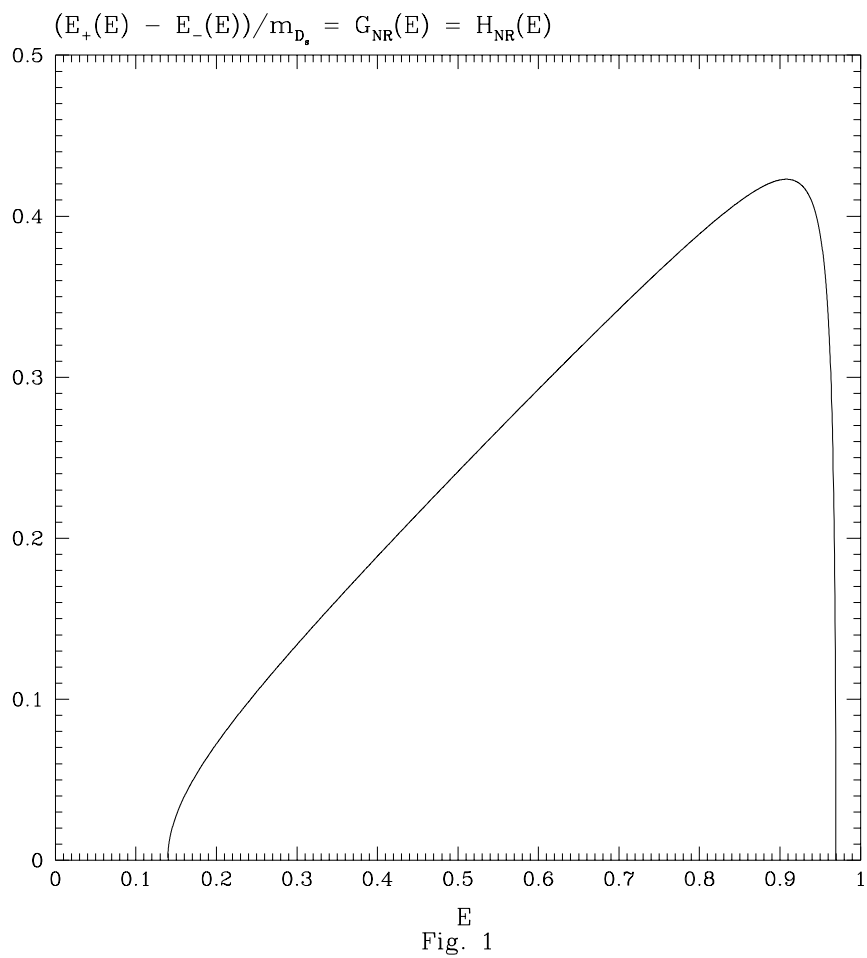


Figure 1: The shape of the pion energy distributions for a uniform Dalitz plot. E stands for E_1 , E_2 , E_3 indifferently.

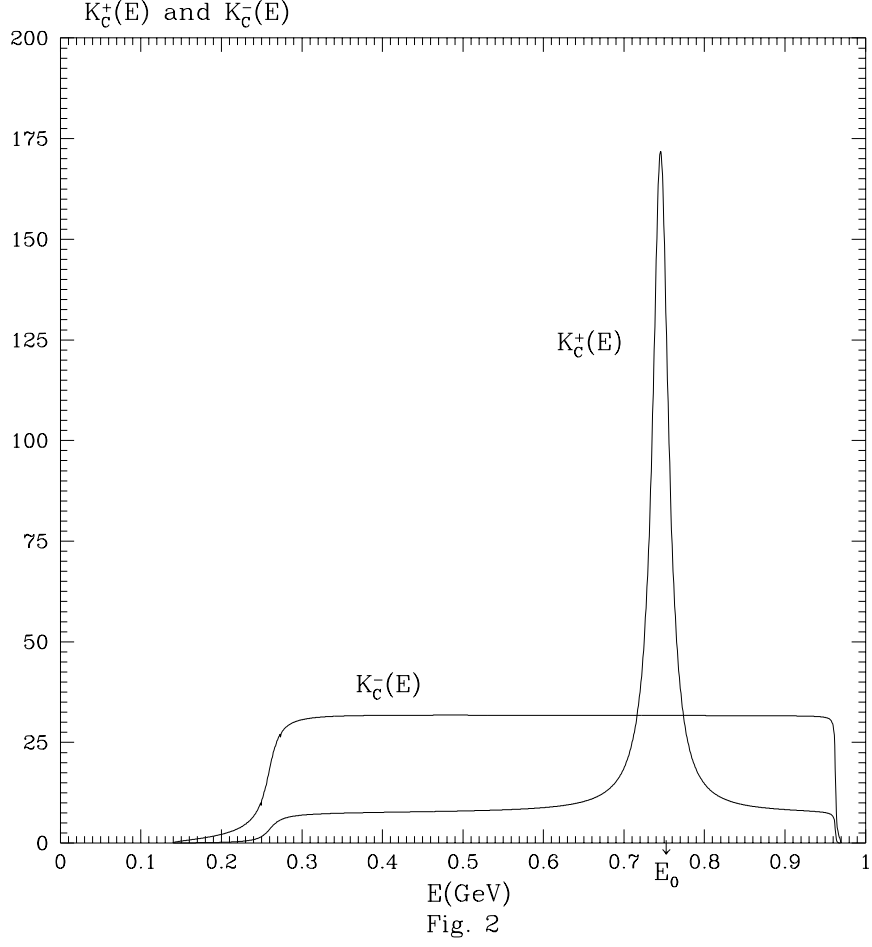


Figure 2: The shapes of the π^+ and π^- meson energy distributions for $D_s^+ \rightarrow f_0 \pi^+ \rightarrow \pi^+ \pi^- \pi^+$. $K_c^+(E)$ represents the energy distributions of π^+ meson, and $K_c^-(E)$ represents that of π^- meson. The quantity $E_0 = 7.45 \text{ GeV}$ is associated to the f_0 resonance.

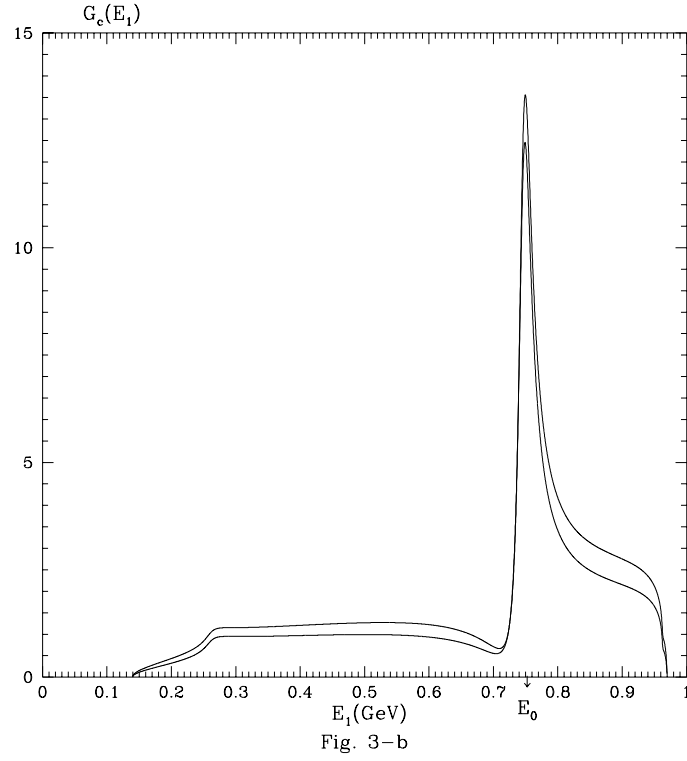
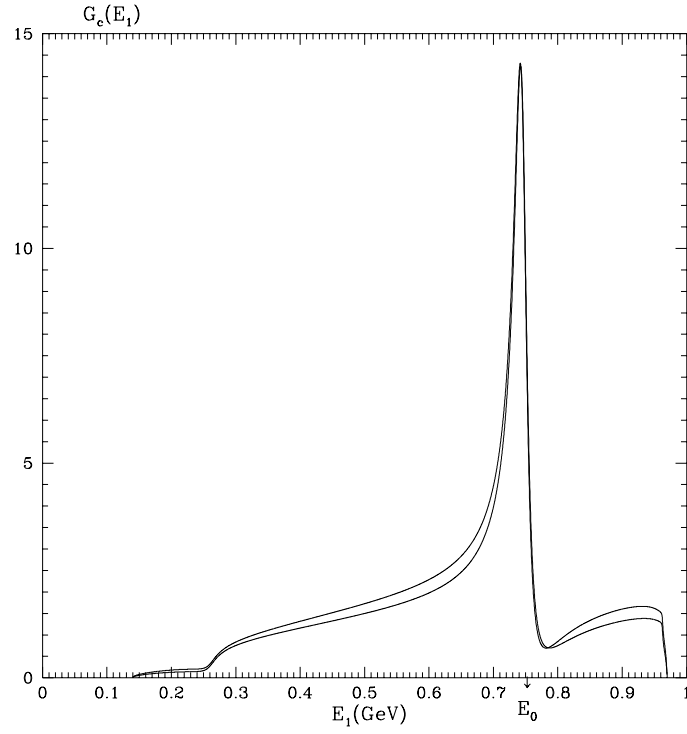


Figure 3: The fully normalized π^+ meson energy distributions for $D_s^+ \rightarrow \pi^+\pi^-\pi^+$. **3-a)** for $\Gamma_{\pi'} = 600 \text{ MeV}$, $1.74 \leq F_{NR} \leq 1.99$, **3-b)** for $\Gamma_{\pi'} = 263 \text{ MeV}$, $-2.07 \leq F_{NR} \leq -1.74$. The two lines in each curve correspond to the extremum values of F_{NR} . The quantity $E_0 = 7.45 \text{ GeV}$ is associated to the f_0 resonance.

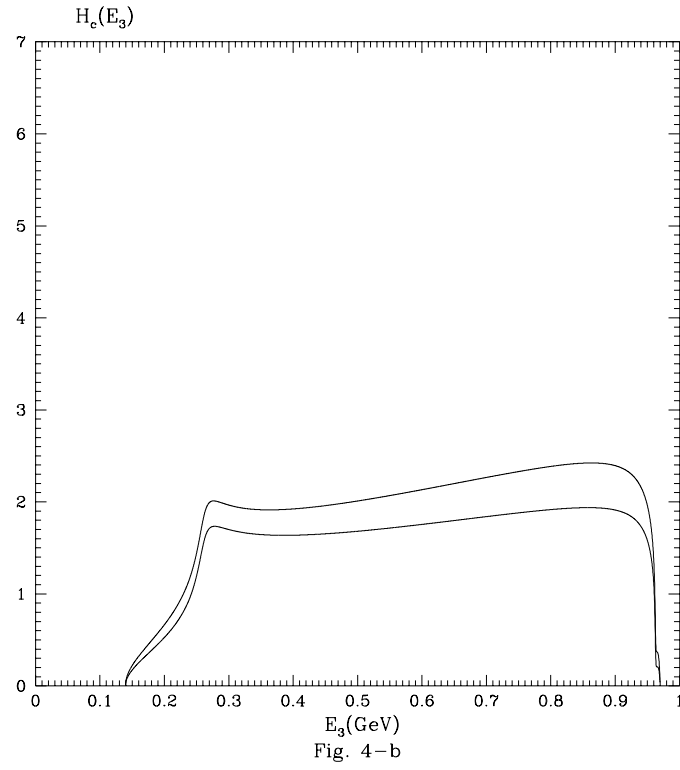
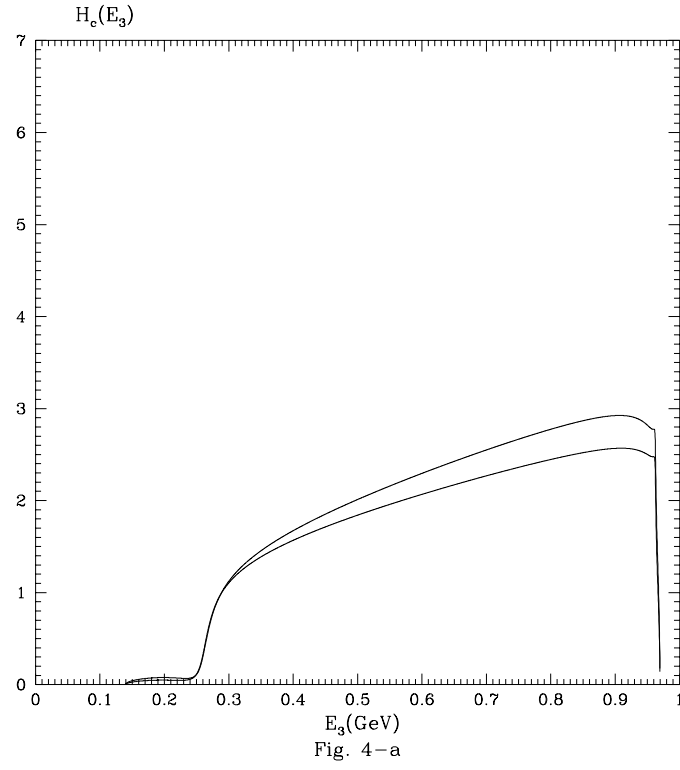


Figure 4: The fully normalized π^- meson energy distributions for $D_s^+ \rightarrow \pi^+ \pi^- \pi^+$. The parameters are the same as in Figure 3.

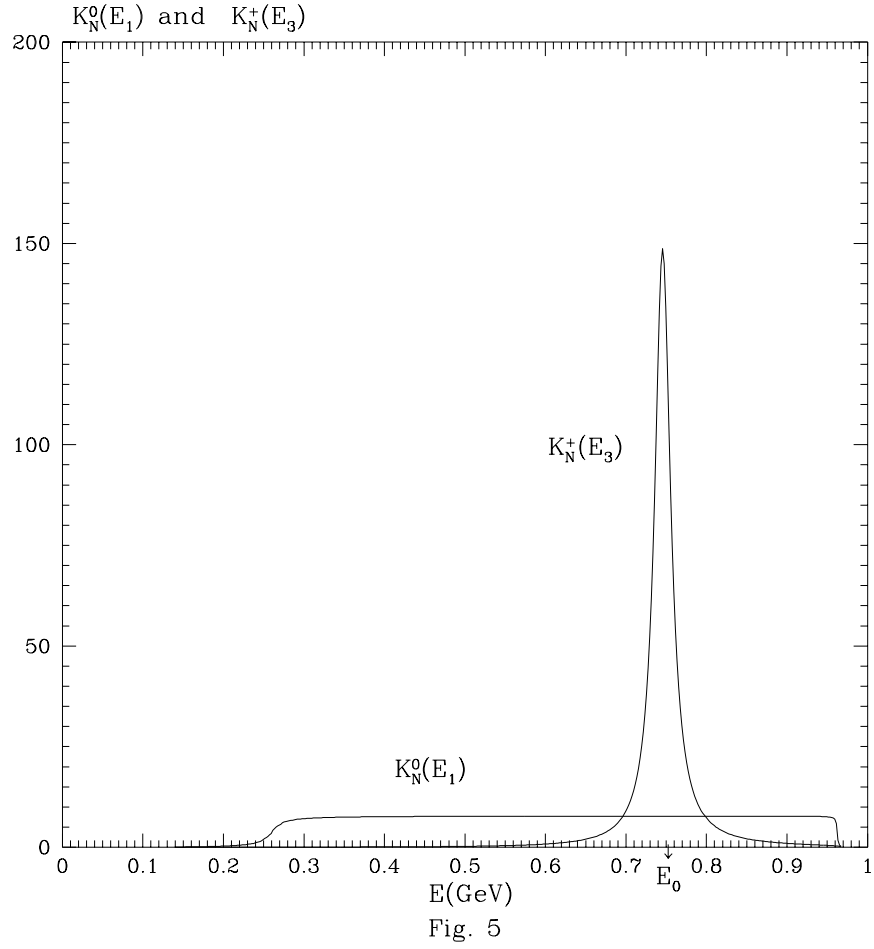


Figure 5: The shapes of the π^0 and π^+ meson energy distributions for $D_s^+ \rightarrow f_0 \pi^+ \rightarrow \pi^0 \pi^0 \pi^+$. The quantity $E_0 = 7.45 \text{ GeV}$ is associated to the f_0 resonance.

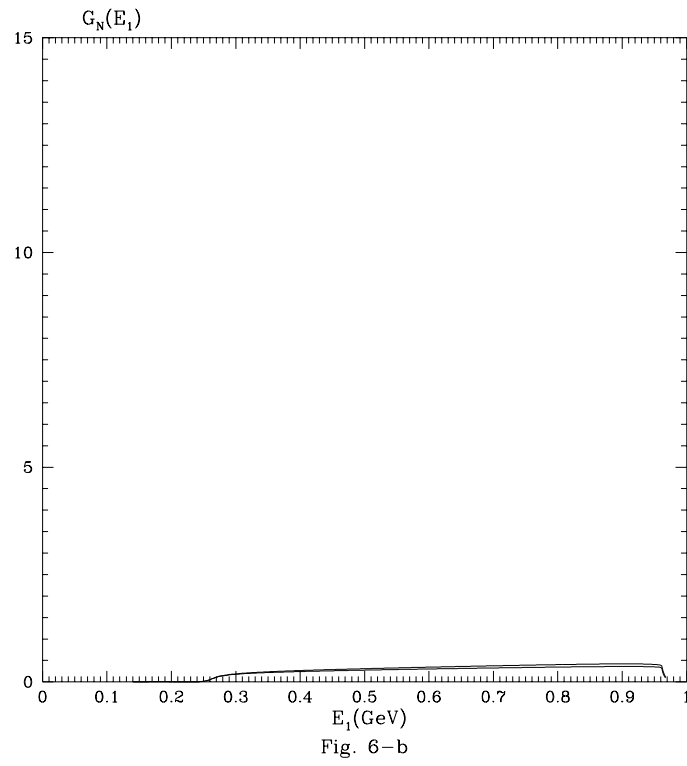
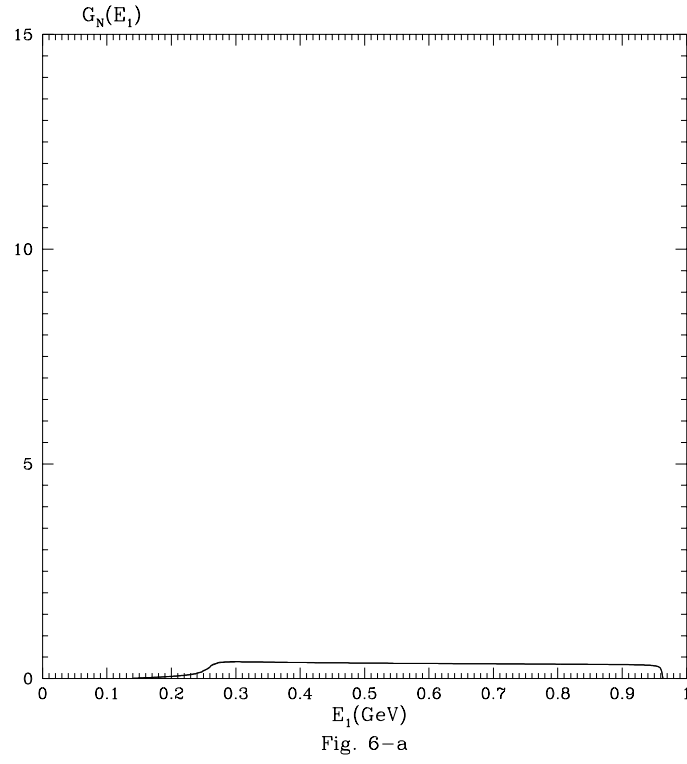


Figure 6: The fully normalized π^0 meson energy distributions for $D_s^+ \rightarrow \pi^0 \pi^0 \pi^+$. The parameters are the same as in Figure 3.

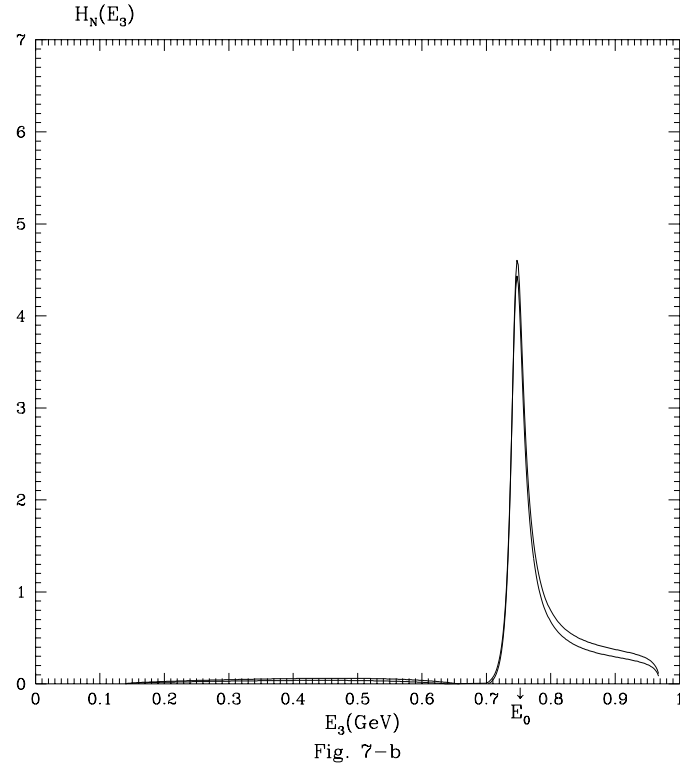
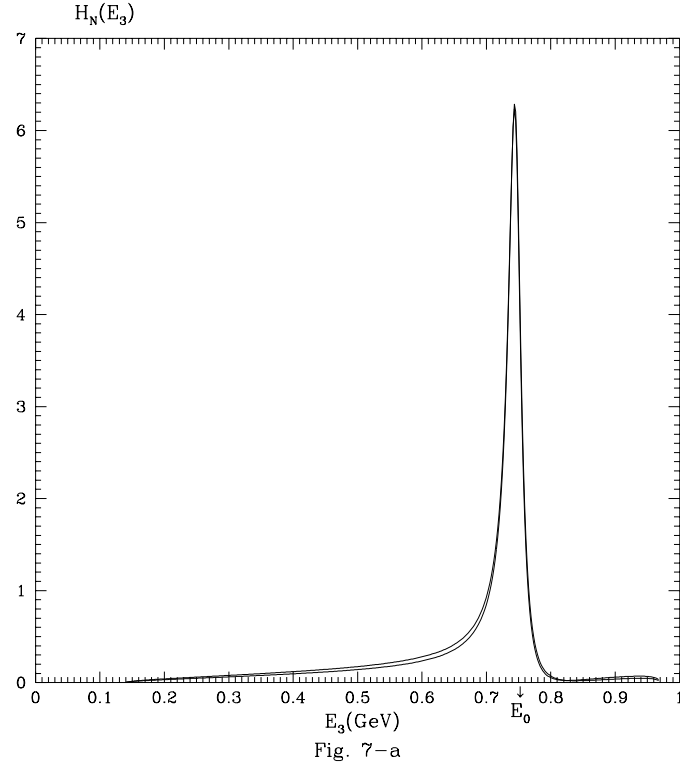


Figure 7: The fully normalized π^+ meson energy distribution for $D_s^+ \rightarrow \pi^0 \pi^0 \pi^+$. The parameters are the same as in Figure 3. The quantity $E_0 = 7.45 \text{ GeV}$ is associated to the f_0 resonance.

This figure "fig1-1.png" is available in "png" format from:

<http://arXiv.org/ps/hep-ph/9503326v1>

This figure "fig1-2.png" is available in "png" format from:

<http://arXiv.org/ps/hep-ph/9503326v1>

This figure "fig1-3.png" is available in "png" format from:

<http://arXiv.org/ps/hep-ph/9503326v1>

This figure "fig1-4.png" is available in "png" format from:

<http://arXiv.org/ps/hep-ph/9503326v1>

This figure "fig1-5.png" is available in "png" format from:

<http://arXiv.org/ps/hep-ph/9503326v1>

This figure "fig1-6.png" is available in "png" format from:

<http://arXiv.org/ps/hep-ph/9503326v1>

This figure "fig1-7.png" is available in "png" format from:

<http://arXiv.org/ps/hep-ph/9503326v1>